Numerical and experimental modelling of internal tide near a continental shelf

Chantal Staquet, Joël Sommeria, Ivane Pairaud, Kaushik Goswami, Mahdi Mohammad Mahdizadeh

Numerical and experimental modelling of the internal tide near a continental shelf

Staquet Chantal, Sommeria Joël, Pairaud Ivane, Goswami Kaushik, Mehdizadeh Mehdi

Laboratoire des Ecoulements Géophysiques et Industriels
CNRS-INPG-UJF
BP 53, Grenoble cédex 9, France
Chantal.Staquet@hmg.inpg.fr

Abstract :

Mixing is an essential process in the deep ocean, as it accounts for the raising of the cold abyssal water masses. The role of internal gravity waves in this process has been questioned because their breaking leads to localized but ubiquitous mixing. The main sources of energy for internal gravity waves are the wind and the interaction of the barotropic tide with the bathymetry. We consider the latter situation in this paper, the internal wave field thus generated being referred to as the internal tide. Joint laboratory and numerical experiments are used to study the internal tide dynamics, in the academic context of a uniformly stratified ocean and when the bathymetry is a two-dimensional continental shelf. We focus on the generation process and on the structure of the internal tide, and briefly address nonlinear effects which occur when the internal tide first reflects from the oceanic bottom.

Résumé :

Les processus de mélange sont essentiels au fond de l'océan car ils permettent la remontée des eaux froides abyssales vers la surface. Une grande question de la communauté océanographique concerne la contribution des ondes internes à ces processus car ces ondes, bien que peu énergétiques en regard des courants marins par exemple, sont présentes partout dans l'océan et y déferlent. Les principales sources d'énergie des ondes internes sont le vent et l'interaction de la marée avec la topographie sous-marine. C'est cette dernière configuration que nous considérons ici, au travers d'expériences de laboratoire et numériques, dans le contexte académique d'un talus continental bidimensionnel dans un océan uniformément stratifié. Nous examinons plus particulièrement le processus de génération du champ d'ondes internes et la structure cinématique de ce champ. Nous discutons également de la manifestation des effets non linéaires lorsque le champ d'ondes se réfléchit au fond de l'océan.

Key-words :

Fluid mechanics; internal gravity waves; ocean mixing.

1 Introduction

Internal gravity waves in the deep ocean have been given much importance for ten years, since Munk & Wunsch (1998) proposed that the raising of the cold abyssal water masses is sustained by the energy sources that feed the mixing processes in the abyss (thereby extending to the open ocean an idea first proposed by Stigebrandt (1979) in fjords). Mixing in the deep ocean is mostly due to breaking gravity waves, which are created by the wind (more precisely, by the interaction of the surface layer due to the wind and the stably-stratified fluid below) and by the interaction of the tide with the bathymetry. The energetic content of both energy sources may be roughly estimated at global scale and are likely to be comparable: the most recent estimates are between 1 TW and 1.5 TW for the wind and about 1 TW for the tide (Wunsch & Ferrari (2004)).

The thermal equilibrium of the deep ocean thus depends upon local, strongly intermittent processes which occur on small temporal scales (of the order of one minute) and small spatial

scales (of the order of ten meters). One may note that, as well, the large scale atmospheric circulation depends upon local mixing processes, which mostly occur in convective clouds (Bony *et al*. (1995)). This gigantic difference in spatial and temporal scales requires the parameterization of the mixing processes (which cannot be ignored as just shown) in large scale circulation models, and even in regional models. This obvious requirement is still an open problem as it relies upon a direct study of the mixing processes. This problem can be tackled via three complementary approaches: (i) a numerical approach, if one has a precise numerical code which solves the full dynamical equations, namely with nonlinear and non hydrostatic terms; (ii) using laboratory experiments, if the dimensions of the experimental device are large enough for the flow dynamics not to be dominated by viscous effects; (iii) via in situ measurements, if the locations where strong mixing occurs can be guessed.

The present paper uses the two first approaches, when the internal gravity waves are forced by the interaction of the tide with the bathymetry. These internal waves are usually referred to as the internal tide. We shall consider the academic situation of a uniformly stratified ocean, when the tide interacts with a simple two-dimensional continental shelf. Numerical experiments have been conducted in close correspondance with the laboratory experiments, the geometrical and physical parameters being the same in both approaches. The laboratory experiments have been performed on the rotating Coriolis platform in Grenoble and are the first laboratory experiments of the internal tide dynamics in a large scale tank (preliminary experiments on a smaller laboratory device have been performed by Gostiaux & Dauxois (2006). We shall focus upon the structure of the internal tide close to its generation region and upon the nonlinear effecs that result from the interaction of the internal tide with the reflected field at the oceanic bottom.

This short paper is naturally organized as follows. The laboratory and numerical experiments are briefly described in the next Section. Results are discussed in Section 3 and conclusions are proposed in the final Section.

2 Laboratory and numerical set-ups

2.1 Laboratory experiments

We force a tidal current over a continental slope, across a channel on the Coriolis rotating platform (see Fig. 1). The barotropic tide is produced by a piston oscillating horizontally, with motion $x = d\cos\omega t$, which closes the channel at one end. The channel is open at the other end to allow free flow of this 'barotropic tide'. A density stratification is initially introduced by salinity when the tank is filled. In the present paper, the values for d and $2\pi/\omega$ are 0.6 cm and 25 s, the Brunt-Vaisala frequency $N = 0.72\text{s}^{-1}$ and the tank is non rotating. This configuration is inspired from the numerical simulations by Gerkema, Staquet & Bouruet-Aubertot Gerkema *et al*. (2006) of the internal tide in the oceanic context, using similarity arguments.

To reach regimes of inertial dynamics, with weak viscous damping, we need a sufficiently deep water (to permit large vertical wavelengths), so we choose a total depth of 90 cm, and a topographic height equal to 75 cm. If this is assumed to represent an ocean 4.5 km deep, the vertical scaling factor is 1/5000. Then the available channel length of 10 m would represent 50 km. This would be limited to the continental slope itself, with no space for internal tide propagation, reflexion and breaking. To simulate the process over a distance of 250 km, we therefore need to apply a distortion of aspect ratio by a factor 5. Hence, the slope will be five times larger in the experiment than in the ocean. Since in the ocean, this slope is close to 0.1, we shall consider a slope close to 0.5, corresponding to an angle with the horizontal of 30^o. We expect that such a distortion does not change the dynamics too much: note that within the hydrostatic approximation, the dynamics is strictly invariant by a change of aspect ratio in the

absence of viscosity effect or turbulence parametrisation.

The main measurement tool is Particle Image Velocimetry (PIV), either in horizontal or vertical planes. Only two cameras can be used simultaneously, so that a choice of the location of the study has to be made: emission zone, reflexion on the bottom, reflexion on the free surface. In addition to PIV, time records of the density at a given point have been obtained, using the vertical profiler with fixed probe position.

2.2 Numerical simulations

The numerical simulations are based on the numerical code developed at MIT by Marshall *et al.* (1997), which we adapted to the experimental configuration. The code solves the nonlinear nonhydrostatic Navier-Stokes equations in the Boussinesq approximation using a finite volume method. The forcing is imposed at the vertical boundary facing the shelf, via an oscillatory velocity field $\dot{x} = d\omega\cos\omega t$, which should not be very different from the oscillating piston of the laboratory experiment since the displacement of the latter is very small. Despite the numerical experiments have been carefully designed so as to fit the laboratory experiments, unavoidable differences still remain. These are the viscous and diffusion effects, which are modelled by a KPP scheme in the numerical simulations. Also, the Prandtl number is equal to 1 in the simulations while the Prandtl number for salt is 700.

The continental slope is solved with 125 grid points (as 700 grid points are used along the horizontal direction) while 160 grid points are used along the vertical direction above the abyssal plain. One tidal period is simulated by 200 time steps.

3 Internal tide propagation

The internal tide propagates as a rectilinear beam in a uniformly stratified fluid, which is tangent to the topography (e.g. Baines (1982)). This behavior is illustrated in Fig. 2a for the experiment and in Fig. 2b for the simulations. It can be accounted for as follows. In a frame of reference attached to the barotropic tide (i.e. to the moving piston, in the experiment, or to the moving lateral boundary, in the simulations), the topography becomes an oscillating body in a uniformly stratified fluid. Assuming this change of reference frame is galilean (see Gerkema (2006) for a discussion), the analysis can be equivalently performed in this new reference frame.

The wave pattern emitted by a spatially bounded oscillating body can be mostly predicted by the dispersion relation, $\cos\theta = \omega/N$, as this implies that the group velocity makes the angle θ with the vertical. The laboratory experiment performed by Mowbray & Rarity (1967) nicely

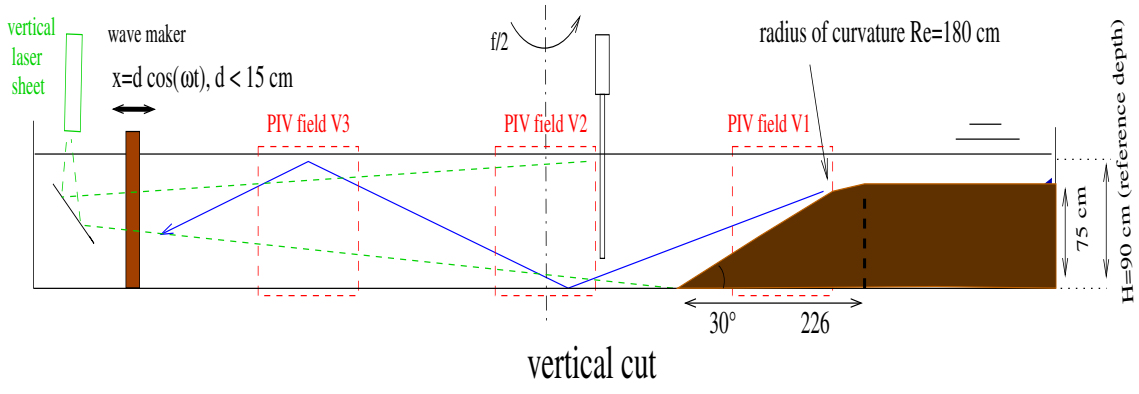

Figure 1: Sketch of the laboratory experiment.

illustrates this relation : the wave pattern recorded in the plane perpendicular to an oscillating horizontal cylinder is made of four beams which are phase lines and along which the energy of the moving cylinder is carried away. The detailed emission pattern also depends upon the typical scale of the oscillating body relative to the amplitude of oscillation (as well as upon unsteady and viscous effects). However, after a sufficient time or, equivalently, at a large enough distance from the source, the beam width is set by this typical scale (this is the diameter of the cylinder for instance). When the oscillating body is not spatially bounded, as this is the case for the topography, numerical and laboratory experiments show that a wave beam forms which extends downwards and upwards from its generation region. The generation region is the location where the tangent to the topography has the same slope as the beam direction. Hence, the beam width should depend upon the radius of curvature at this location. But the precise dependence of this width upon the geometrical and physical parameters of the problem is still an open question.

The beam width can be estimated from the experiments by plotting the velocity field along the beam U as a function of the distance perpendicular to the beam η. This profile is plotted at successive times during one tidal period in Fig. 3a for the laboratory experiment and in Fig. 3b for the numerical experiment. The superposition of the profiles displays the envelope of the beam, from which the beam width can be inferred. It is noteworthy that the maximum amplitude of the envelope is quite close in the numerical and laboratory experiments, being approximately equal to 0.6 cm/s. The envelope of the beam seems actually to have two local maxima, the origin of which is not clear yet. Another local maximum appears further away from the beam, which may be attributed to transients leaving the domain (B. Voisin, private comm.).

In addition to the width, the beam involves another scale which is the wavelength. The latter scale is actually ill-defined because the wave field is not monochromatic inside the beam. It is still noteworthy that, when the velocity field $U(\eta)$ is plotted at two successive times distant by half a tidal period, the two profiles are out-of-phase (Fig. 4a). This suggests that the wave structure is locally monochromatic inside the beam. This can be attested by plotting the maximum and minimum value of $U(\eta)$ as a function of time over one period. The monochromatic character should yield a linear behavior, whereof slope defines a local phase speed, from which a wavelength can be defined. Fig. 4b shows that this indeed the case and that the wavelength is of the same order as the beam width.

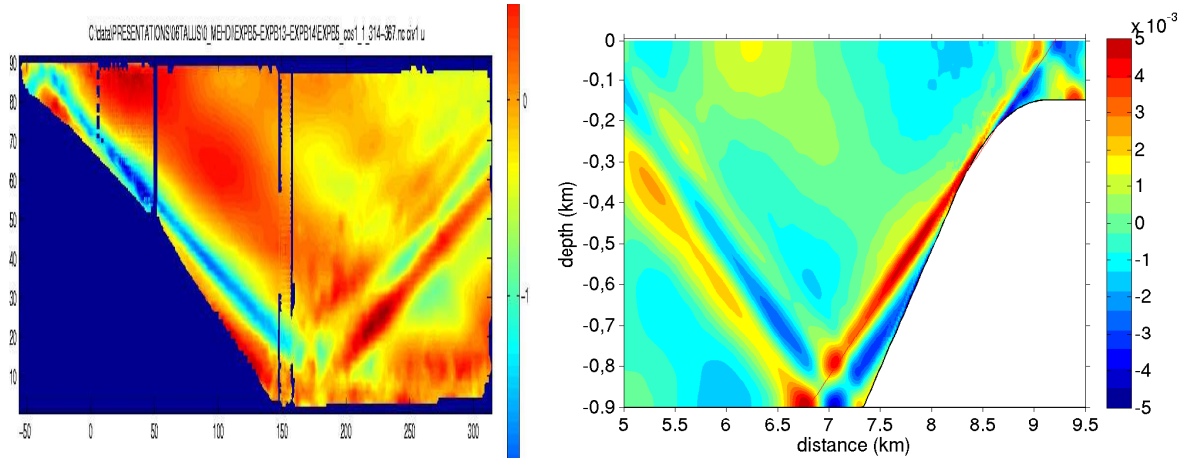

(a) (b)

Figure 2: (a) Laboratory experiment. Spatial distribution of the horizontal velocity component filtered at the tidal frequency (i.e. $u\cos(\omega.t)$ averaged over the 5th and 6th tidal periods); (b) Numerical experiment. Same as (a) for an average performed over the 11th and 12th tidal periods.

4 Internal tide reflection: nonlinear effects

The superposition of the incident and reflected beams at the flat bottom boundary leads nonlinear interaction between the two beams. As a result, internal waves with higher harmonics are produced, as shown in the numerical simulations of Gerkema *et al*. (2006). The laboratory experiments also clearly reproduce this nonlinear behavior, as shown in Fig. 5.

5 Conclusions

This short paper provides preliminary results from the first laboratory experiment of the internal tide on a large enough experimental device for an inertial dynamics to be reached. Results from

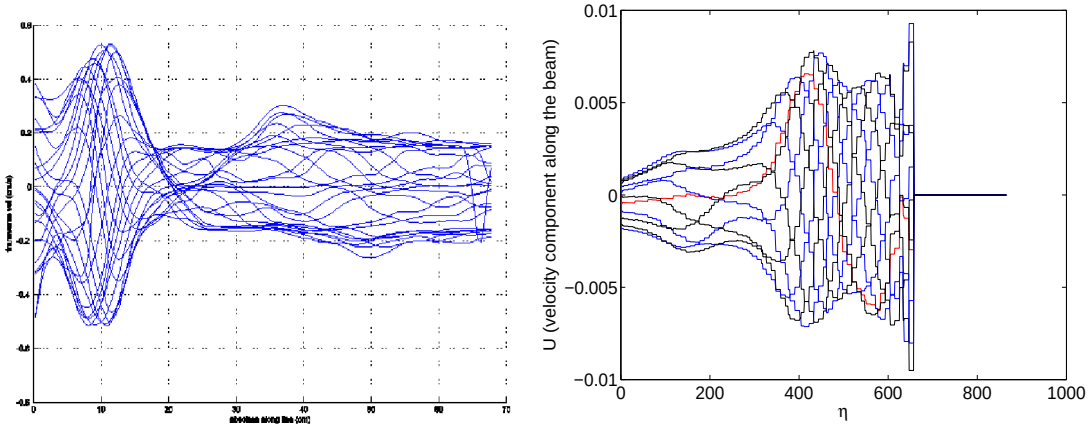

(a) (b)

Figure 3: (a) Laboratory experiment. Velocity component along the beam as a function of the distance perpendicular to the beam, at successive times during the 5th tidal period. (b) Numerical experiment. Same as (a) during the 11th tidal period.

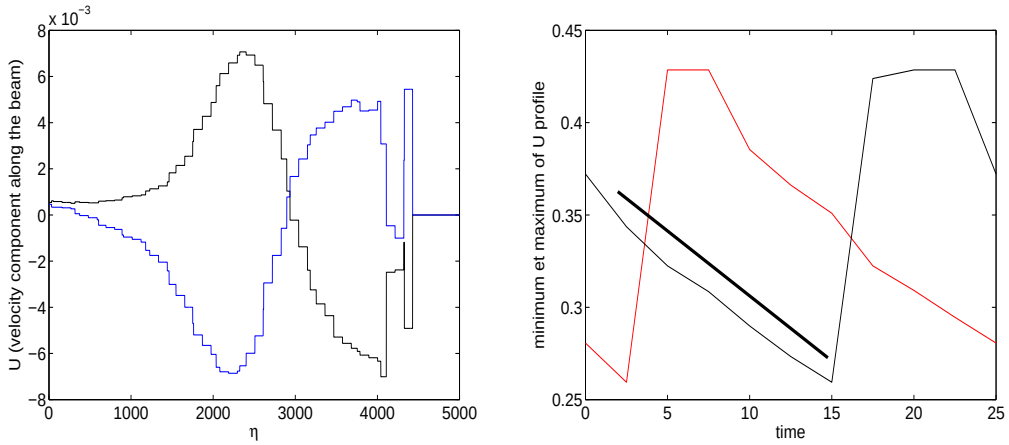

(a) (b)

Figure 4: Numerical experiment. (a) Velocity component along the beam as a function of the distance perpendicular to the beam, at two times separated by half a tidal period. (b) Maximum and minimum value of this velocity component as a function of time. The slope of the thick line is an estimate of the phase velocity inside the beam.

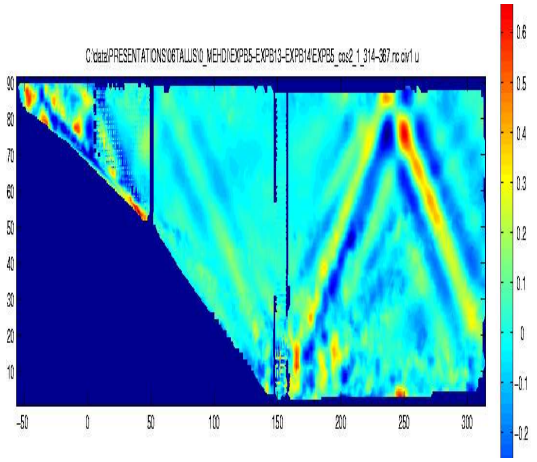

Figure 5: Laboratory experiment. Spatial distribution of the horizontal velocity component filtered at twice the tidal frequency (i.e. $u\cos(2\omega.t)$ averaged over the 5th and 6th tidal periods).

a carefully designed numerical experiment, which matches as much as possible the geometrical and physical parameters of the laboratory experiment, are also presented. Further work is under progress, in order to analyse the influence of rotation upon the generation of harmonics, the influence of a thermocline on the internal tide propagation and, more generally, processes leading to the loss of energy from the coherent internal tide which emerges from the topography.

Acknowledgements

This research is supported by contract no ANR-05-BLAN-0176-01. Computations have been performed on the machines of the supercomputer centre IDRIS under contract no 060580.

References

P Baines. On internal tide generation models. *Deep-Sea Research*, 29:307–338, 1982.

S. Bony, J. P. Duvel, and H. Le Treut. Observed dependence of the water vapor and clear-sky greenhouse effect on sea surface temperature: comparison with climate warming experiments. *Climate Dynamics*, 11:307–320, 1995.

T. Gerkema. Internal-wave reflection from uniform slopes: higher harmonics and coriolis effects. *Nonlinear Processes in Geophysics (submitted)*, 2006.

T. Gerkema, C. Staquet, and P. Bouruet-Aubertot. Nonlinear effects in internal tide beams and mixing. *Ocean Modelling*, 12:302–318, 2006.

L. Gostiaux and T. Dauxois. Internal tides in laboratory experiments. *Physics Fluids (submitted)*, 2006.

J. Marshall, A. Adcroft, C. Hill, L. Perelman, and C. Heisey. A finite-volume, incompressible navier-stokes model for studies of the ocean on parallel computers. *Journ. Geophys. Res.*, 102:5753–5766, 1997.

D. E. Mowbray and B. S. H. Rarity. The internal wave pattern produced by a sphere moving vertically in a density stratified liquid. *J. Fluid Mech.*, 30:489–495, 1967.

W. Munk and C. Wunsch. Abyssal recipes ii: energetics of tidal mixing and wind mixing. *Deep Sea Research I*, 45:1977–2010, 1998.

A. Stigebrandt. Observational evidence for vertical diffusion driven by internal waves of tidal origin in the oslo fjord. *Journ. Phys. Ocean.*, 9:435–441, 1979.

C. Wunsch and R. Ferrari. Vertical mixing, energy, and the general circulation of the oceans. *Annual Review of Fluid Mechanics*, 36:281–314, 2004.